

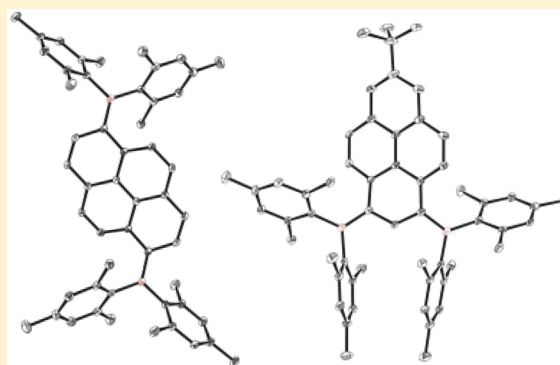
Bis(boryl anion)-Substituted Pyrenes: Syntheses, Characterizations, and Crystal Structures

Ningning Yuan, Wenqing Wang, Yong Fang, Jiacheng Zuo, Yue Zhao, Gengwen Tan,^{*ID} and Xinping Wang^{*ID}

State Key Laboratory of Coordination Chemistry, School of Chemistry and Chemical Engineering, Collaborative Innovation Center of Advanced Microstructures, Nanjing University, Nanjing 210023, People's Republic of China

Supporting Information

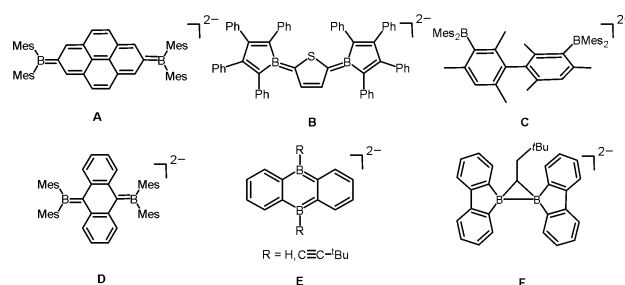
ABSTRACT: The two new diboranes **1** and **2** connected by a pyrene moiety at the 1,6- and 1,3-positions, respectively, were synthesized, and their two-electron-reduction reactions were investigated. The doubly reduced species **1**^{••2-} is silent in electron paramagnetic resonance (EPR) and nuclear magnetic resonance (NMR) spectroscopic measurements, suggesting a quasi-quinoidal structure with a diradical character of **1**^{••2-}, which has a singlet–triplet gap of 6.6 kcal mol⁻¹ as determined by theoretical calculations. In contrast, the reduction product **2**^{••2-} is EPR active and theoretical calculations indicate that **2**^{••2-} has an open-shell singlet ground state with a singlet–triplet energy gap of 4.9 kcal mol⁻¹.



The synthesis of stable main-group-element-based radicals represents one of the most active research fields in contemporary organometallic chemistry.¹ Diradicals, molecules with two unpaired electrons, have been attracting a great deal of attention in the last decades owing to their importance in understanding the nature of the chemical bonds and their interesting physical properties (optical, electronic, magnetic, etc.).² They are envisioned to have promising applications as functional materials in electronic devices, quantum information processing systems, and organic spintronics.² Three-coordinate boranes have proven to be elegant spin carriers, and they have been frequently utilized to construct diradicals owing to their intrinsic electron deficiency.³ For instance, Kaim and co-workers demonstrated that 1,4-phenylene- and 4,4'-diphenylene-linked diboranes could undergo one-electron reduction, affording their radical anions as detected in situ by EPR spectroscopy.^{3a} Rajca and co-workers reported a persistent bis(boryl anion) diradical in solution featuring a triplet ground state, but its solid state structure was not determined.⁴ Since then, with the help of sterically encumbered and π -conjugated ligands, stable boron-based monoradicals, stabilized by delocalization of the unpaired electron on one or more boron atoms, have been isolated,⁵ and diboryl dianions **A**–**F** have been isolated and fully characterized (Scheme 1).

The dianions **A**⁵¹ and **B**⁶ feature an open-shell singlet ground state as indicated by theoretical calculations, while **D**–**F**^{5m,7} have closed-shell structures. In addition, we recently reported the first example of stable bis(boryl anion) diradical **C** having a triplet ground state with a small singlet–triplet energy gap.⁸ These results suggest that the bridging unit can tune the property of the obtained diradical dianion species of diborane,

Scheme 1. Structurally Characterized Diboryl Dianions



reminiscent of the scenario observed in bis(triarylamine)-based diradical dications.⁹

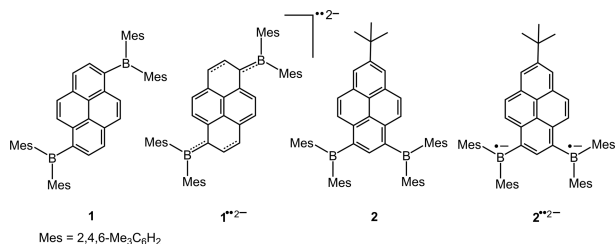
Pyrene-based materials have widely applied as organic electronics, and a variety of pyrene derivatives have been synthesized up to now.¹⁰ The substitution of pyrene at different positions of pyrene rings renders its derivatives significantly different properties. Tethering two Mes₂B units to pyrene moiety at 2,7-positions followed by two-electron reduction afforded the dianion **A**, which has some biradicaloid character with a singlet–triplet energy gap of 13 kcal mol⁻¹ as determined by computational calculations.⁵¹ In order to investigate how the Mes₂B functional groups at the different positions of pyrene can influence the electronic structures of

Special Issue: Tailoring the Optoelectronic Properties of Organometallic Compounds with Main Group Elements

Received: May 12, 2017

the corresponding doubly reduced species, we synthesized the precursors **1** and **2** with two Mes₂B moieties at the 1,6- and 1,3-positions, respectively (Scheme 2). Herein, we report two-

Scheme 2. Pyrene-Bridged Diboranes **1** and **2** and Their Doubly Reduced Species



electron reduction of **1** and **2** affording the isolable diradical dianions **1**^{••2••-} and **2**^{••2••-}, respectively, with significantly smaller singlet–triplet gaps in comparison to that of **A**.⁵¹

The neutral compounds **1** and **2** were synthesized by the reactions of Mes₂BF with 1/2 molar equiv of the corresponding dilithium salts of pyrene, which were generated in situ through transmetalation of the dibromopyrene precursors with 2 molar equiv of *n*BuLi in THF (see the Supporting Information for details). Compounds **1** and **2** were isolated as yellow solids, and they were characterized by NMR spectroscopy and elemental analysis. The cyclic voltammetry investigation of **1** and **2** revealed two nearly reversible reduction peaks at −2.24, −1.95 V and at −2.41, −1.89 V, versus the Ag/Ag⁺ reference electrode (Figures S1 and S2 in the Supporting Information), respectively, suggesting that their doubly reduced species might be stable enough for isolation.

Encouraged by the electrochemical reduction results, we further carried out two-electron chemical reduction of **1** and **2** in an attempt to isolate their doubly reduced species and study their structural and electronic properties. The reduction of **1** and **2** with a slight excess amount of K₂C₈ in the presence of 18-crown-6 in THF at room temperature afforded the doubly reduced dianion salts [(18-c-6)K(THF)₂]₂⁺·**1**^{••2••-} and [(18-c-6)K(THF)₂]₂⁺·**2**^{••2••-} as blue crystals in 19.8% and 20.1% yields, respectively. The molecular structures and electronic structures of **1**^{••2••-} and **2**^{••2••-} were further studied by X-ray crystallography, EPR spectroscopy, and UV–vis absorption spectroscopy, in conjunction with DFT calculations.

The dianion salt [(18-c-6)K(THF)₂]₂⁺·**1**^{••2••-} crystallizes in the triclinic space group *P* $\bar{1}$. The structure of **1**^{••2••-} is shown in Figure 1, it possesses a crystallographic inversion center in the crystal. The dianion of [(18-c-6)K(THF)₂]₂⁺·**2**^{••2••-} is shown in Figure 2, there are two essentially identical molecules in the same asymmetric unit. In contrast to the perfectly planar geometry of the central moiety in **A**, the two boron atoms in **1**^{••2••-} and **2**^{••2••-} are not in the same plane with the central pyrene moiety, and they reside at two different sides of the pyrene plane (Figures 1b and 2b). The boron centers have an almost planar configuration with the sum of angles around boron atoms being 359.7° in **1**^{••2••-} and 359.5 and 359.6° in **2**^{••2••-}. The dihedral angles between the BC₃ and pyrene planes are 27.83° in **1**^{••2••-} and 33.74 and 30.23° in **2**^{••2••-}. The B–C(pyrene) bonds (1.500(4) Å in **1**^{••2••-} and 1.504(7) and 1.504(6) Å in **2**^{••2••-}) are slightly shorter than those in **A** (1.510(3) Å)⁵¹ but much longer than those in **D** (1.486(7) and 1.483(6) Å).^{5m} In **1**^{••2••-}, the C–C bonds d and g–k in the central six-membered ring have the property of aromatic C–C

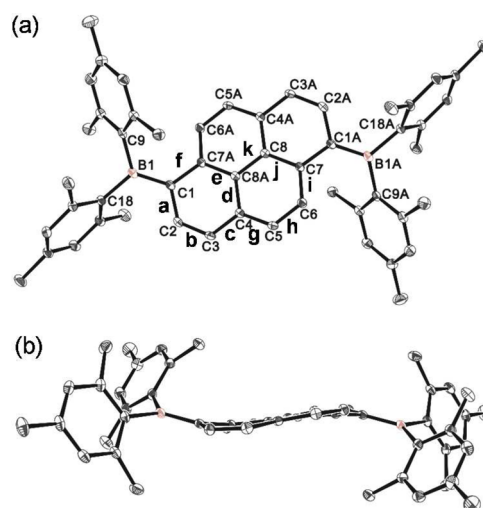


Figure 1. Top view of the molecular structure of the diradical dianion **1**^{••2••-} (a) and its side view (b). All hydrogen atoms are omitted for clarity. Selected bond lengths (Å) and angles (deg): B1–C1 1.500(4), B1–C9 1.608(5), B1–C18 1.619(4), C1–C2 1.440(4), C1–C7A 1.474(4), C2–C3 1.358(4), C3–C4 1.440(4), C4–C5 1.392(4), C5–C6 1.392(4), C6–C7 1.399(4), C7–C8 1.437(4), C4–C8A 1.435(4), C8–C8A 1.435(5); C1–B1–C9 122.7(3), C1–B1–C18 120.1(3), C9–B1–C18 116.9(3).

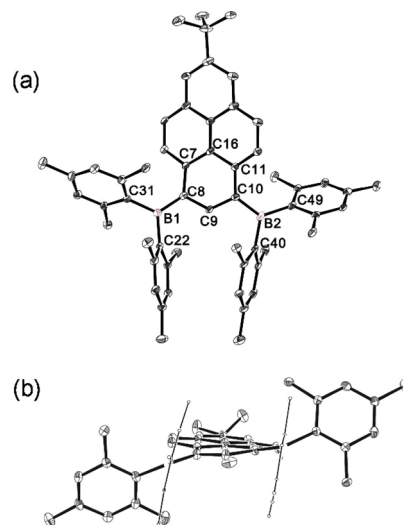


Figure 2. Top view of the molecular structure of the diradical dianion **2**^{••2••-} (a) and its side view (b). All hydrogen atoms are omitted, and two Mes moieties are drawn in a wireframe mode for the sake of clarity. Selected bond lengths (Å) and angles (deg): B1–C8 1.504(7), B1–C22 1.620(7), B1–C31 1.612(7), B2–C10 1.504(6), B2–C49 1.602(7), B2–C40 1.609(7), C7–C8 1.471(6), C8–C9 1.416(6), C9–C10 1.391(6), C10–C11 1.480(6), C7–C16 1.429(7), C11–C16 1.432(6); C8–B1–C22 119.9(4), C8–B1–C31 122.4(4), C22–B1–C31 117.2(4), C10–B2–C49 125.1(4), C10–B2–C40 116.3(4), C49–B2–C40 118.2(4).

bonds, whereas the bond b is more typical of a C=C double bond (1.360(4) Å). Therefore, **1**^{••2••-} is best described as a naphthalene substituted by two boron analogues of butadiene at the 1,8- and 4,6-positions as shown in Scheme 2, which is strikingly different from the structure of **A**.⁵¹ The C–C bonds of the pyrene group in **2**^{••2••-} feature an aromatic C–C bond property, indicating limited electron delocalization over the pyrene moiety.

In order to elucidate the electronic structures of $1^{\bullet\bullet 2-}$ and $2^{\bullet\bullet 2-}$, we further carried out EPR measurements and theoretical calculations. The microcrystalline sample of $1^{2-\bullet\bullet}$ is EPR silent at both room temperature and low temperatures, suggesting a diamagnetic nature or relatively large singlet–triplet gap. Comparison of the calculated energies at the upbe1pbe/6-31G* level indicates that the open-shell singlet (OS) state has the lowest energy with a OS–triplet gap of 6.6 kcal mol^{−1} after an approximate spin projection (AP) method treatment.¹¹ Moreover, the THF solution of $1^{\bullet\bullet 2-}$ is also NMR silent at room temperature and at 213 K except for the observation of the proton signals of 18-c-6.¹² Therefore, $1^{2-\bullet\bullet}$ is best described as a dianion with some diradical character, similar to that of A.⁵¹

In contrast, the crystalline sample of $2^{\bullet\bullet 2-}$ is EPR active and a quite broad resonance signal was observed along with a weak $\Delta m_s = \pm 2$ (half-field) transition at 90 K (Figure 3a), suggesting

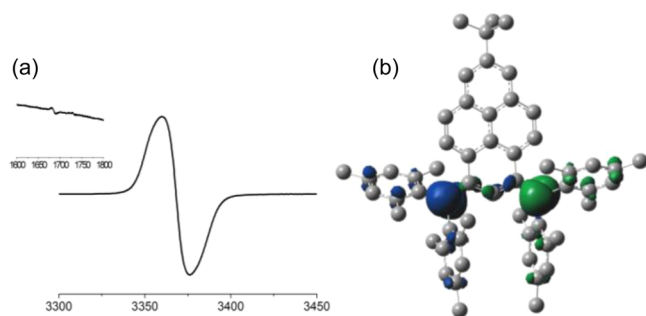


Figure 3. (a) EPR spectrum of $[(18\text{-c-}6)\text{K}(\text{THF})_2]^+ \cdot 2^{\bullet\bullet 2-}$ at 90 K in the solid state. The inset shows the half-field signal. (b) Mulliken spin density distribution of $2^{\bullet\bullet 2-}$ in an open-shell singlet state.

a spin-triplet state of $2^{\bullet\bullet 2-}$.¹³ Variable-temperature EPR measurements reveal a good linear correlation of $\ln(AT)$ versus $1/T$, where A is the absorption area of the half-field signal, yielding a singlet–triplet gap of 4.8 kcal mol^{−1} (Figure S3 in the Supporting Information).¹⁴ DFT calculations reveal that the open-shell singlet is the ground state, and the singlet–triplet gap is 4.9 kcal mol^{−1} after applying an AP method treatment,¹¹ in accordance with the experimental result. Moreover, the Mulliken spin density distribution indicates that the spin density is mainly localized on two boron centers with a small amount on the pyrene group (Figure 3b).

The UV–vis absorption spectra of **1**, **2**, $1^{\bullet\bullet 2-}$, and $2^{\bullet\bullet 2-}$ were obtained in THF under a nitrogen atmosphere (Figure 4). In comparison to their neutral precursors, there are three long-

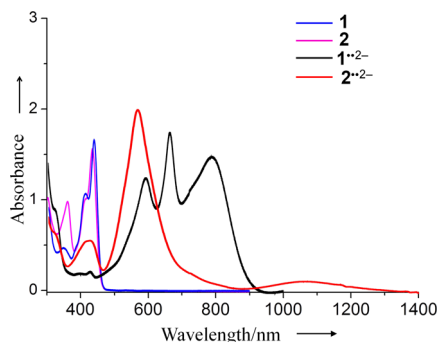


Figure 4. UV–vis spectra of **1**, **2**, $[(18\text{-c-}6)\text{K}(\text{THF})_2]^+ \cdot 1^{\bullet\bullet 2-}$, and $[(18\text{-c-}6)\text{K}(\text{THF})_2]^+ \cdot 2^{\bullet\bullet 2-}$ (1×10^{-4} M) in THF at room temperature.

wavelength absorptions (589, 659, and 787 nm) for $1^{2-\bullet\bullet}$ and two absorptions (569 and 1066 nm) for $2^{\bullet\bullet 2-}$ present in the corresponding spectra. The absorptions at 787 and 1066 nm for $1^{\bullet\bullet 2-}$ and $2^{\bullet\bullet 2-}$, respectively, attributed to the SOMO–LUMO transition according to time-dependent DFT calculations (Figures S4–S7 in the Supporting Information).

In summary, we have demonstrated that, by changing the substitution positions of the diboryl groups from the 1,6- to the 1,3-positions of pyrene moiety, the electronic structures of the obtained dianion $1^{\bullet\bullet 2-}$ and $2^{\bullet\bullet 2-}$ are strikingly different. $1^{\bullet\bullet 2-}$ features a singlet ground state and can be treated as a naphthalene moiety substituted by two boron analogues of butadiene at the 1,8- and 4,6-positions. The dianion $2^{\bullet\bullet 2-}$ is EPR active, and it has an open-shell singlet ground state as determined by theoretical calculations and variable-temperature EPR spectroscopy. Our work demonstrates that the singlet–triplet gap of bis(boryl anion) diradicals can be tuned facilely by changing the substitution positions at the bridging unit.

■ ASSOCIATED CONTENT

Supporting Information

The Supporting Information is available free of charge on the ACS Publications website at DOI: 10.1021/acs.organo-met.7b00368.

Experimental details, crystallographic data, cyclic voltammograms of **1** and **2**, and DFT calculation details (PDF) Cartesian coordinates for the calculated structures (XYZ)

Accession Codes

CCDC 1548469–1548470 contain the supplementary crystallographic data for this paper. These data can be obtained free of charge via www.ccdc.cam.ac.uk/data_request/cif, or by emailing data_request@ccdc.cam.ac.uk, or by contacting The Cambridge Crystallographic Data Centre, 12 Union Road, Cambridge CB2 1EZ, UK; fax: +44 1223 336033.

■ AUTHOR INFORMATION

Corresponding Authors

*E-mail for G.T.: gengwentan@126.com.

*E-mail for X.W.: xpwang@nju.edu.cn.

ORCID

Gengwen Tan: 0000-0002-6972-2197

Xinping Wang: 0000-0002-1555-890X

Notes

The authors declare no competing financial interest.

■ ACKNOWLEDGMENTS

We thank the National Natural Science Foundation of China (Grant 21525102, X.W.; Grant 21601082, G.T.), the Major State Basic Research Development Program (Grant 2016YFA0300404, X.W.), and the Natural Science Foundation of Jiangsu Province (Grant BK20140014, X.W.) for financial support. We are grateful to the High Performance Computing Center of Nanjing University for doing the numerical calculations in this paper on its IBM Blade cluster system. G.T. acknowledges the National Postdoc Foundation for a fellowship. N.Y. thanks the Promotion B project of Nanjing University for a scholarship.

■ REFERENCES

- (1) (a) Power, P. P. *Chem. Rev.* **2003**, *103*, 789. (b) Chivers, T.; Konu, J., In *Comprehensive Inorganic Chemistry II*; 2nd ed.;

- Poeppelmeier, K., Ed.; Elsevier: Amsterdam, 2013; p 349. (c) Martin, C. D.; Soleilhavoup, M.; Bertrand, G. *Chem. Sci.* **2013**, *4*, 3020. (d) Chandra Mondal, K.; Roy, S.; Roesky, H. W. *Chem. Soc. Rev.* **2016**, *45*, 1080.
- (2) (a) Rajca, A. *Chem. Rev.* **1994**, *94*, 871. (b) Breher, F. *Coord. Chem. Rev.* **2007**, *251*, 1007. (c) Abe, M.; Ye, J.; Mishima, M. *Chem. Soc. Rev.* **2012**, *41*, 3808. (d) Abe, M. *Chem. Rev.* **2013**, *113*, 7011. (e) Zeng, Z.; Shi, X.; Chi, C.; Lopez Navarrete, J. T.; Casado, J.; Wu, J. *Chem. Soc. Rev.* **2015**, *44*, 6578.
- (3) (a) Kaim, W.; Schulz, A. *Angew. Chem., Int. Ed. Engl.* **1984**, *23*, 615. (b) Fiedler, J.; Zališ, S.; Klein, A.; Hornung, F. M.; Kaim, W. *Inorg. Chem.* **1996**, *35*, 3039. (c) Kaim, W.; Hosmane, N. S.; Zališ, S.; Maguire, J. A.; Lipscomb, W. N. *Angew. Chem., Int. Ed.* **2009**, *48*, 5082. (d) Ji, L.; Griesbeck, S.; Marder, T. B. *Chem. Sci.* **2017**, *8*, 846.
- (4) Rajca, A.; Rajca, S.; Desai, S. R. *J. Chem. Soc., Chem. Commun.* **1995**, 1957.
- (5) (a) Olmstead, M. M.; Power, P. P. *J. Am. Chem. Soc.* **1986**, *108*, 4235. (b) Grigsby, W. J.; Power, P. P. *Chem. Commun.* **1996**, 2235. (c) Grigsby, W. J.; Power, P. P. *Chem. - Eur. J.* **1997**, *3*, 368. (d) Chiu, C.-W.; Gabbai, F. P. *Angew. Chem., Int. Ed.* **2007**, *46*, 1723. (e) Aramaki, Y.; Omiya, H.; Yamashita, M.; Nakabayashi, K.; Ohkoshi, S.-i.; Nozaki, K. *J. Am. Chem. Soc.* **2012**, *134*, 19989. (f) Braunschweig, H.; Dyakonov, V.; Jimenez-Halla, J. O. C.; Kraft, K.; Krummenacher, I.; Radacki, K.; Sperlich, A.; Wahler, J. *Angew. Chem., Int. Ed.* **2012**, *51*, 2977. (g) Kushida, T.; Yamaguchi, S. *Organometallics* **2013**, *32*, 6654. (h) Bissinger, P.; Braunschweig, H.; Damme, A.; Krummenacher, I.; Phukan, A. K.; Radacki, K.; Sugawara, S. *Angew. Chem., Int. Ed.* **2014**, *53*, 7360. (i) Hübner, A.; Diehl, A. M.; Diefenbach, M.; Endeward, B.; Bolte, M.; Lerner, H.-W.; Holthausen, M. C.; Wagner, M. *Angew. Chem., Int. Ed.* **2014**, *53*, 4832. (j) Bissinger, P.; Braunschweig, H.; Damme, A.; Hörl, C.; Krummenacher, I.; Kupfer, T. *Angew. Chem., Int. Ed.* **2015**, *54*, 359. (k) Hübner, A.; Kaese, T.; Diefenbach, M.; Endeward, B.; Bolte, M.; Lerner, H.-W.; Holthausen, M. C.; Wagner, M. *J. Am. Chem. Soc.* **2015**, *137*, 3705. (l) Ji, L.; Edkins, R. M.; Lorbach, A.; Krummenacher, I.; Brückner, C.; Eichhorn, A.; Braunschweig, H.; Engels, B.; Low, P. J.; Marder, T. B. *J. Am. Chem. Soc.* **2015**, *137*, 6750. (m) Zheng, Y.; Xiong, J.; Sun, Y.; Pan, X.; Wu, J. *Angew. Chem., Int. Ed.* **2015**, *54*, 12933. (n) Yuan, N.; Wang, W.; Wu, Z.; Chen, S.; Tan, G.; Sui, Y.; Wang, X.; Jiang, J.; Power, P. P. *Chem. Commun.* **2016**, *52*, 12714.
- (6) Braunschweig, H.; Dyakonov, V.; Engels, B.; Falk, Z.; Hörl, C.; Klein, J. H.; Kramer, T.; Kraus, H.; Krummenacher, I.; Lambert, C.; Walter, C. *Angew. Chem., Int. Ed.* **2013**, *52*, 12852.
- (7) (a) Lorbach, A.; Bolte, M.; Lerner, H.-W.; Wagner, M. *Organometallics* **2010**, *29*, 5762. (b) von Grotthuss, E.; Diefenbach, M.; Bolte, M.; Lerner, H.-W.; Holthausen, M. C.; Wagner, M. *Angew. Chem., Int. Ed.* **2016**, *55*, 14067.
- (8) Wang, L.; Fang, Y.; Mao, H.; Qu, Y.; Zuo, J.; Zhang, Z.; Tan, G.; Wang, X. *Chem. - Eur. J.* **2017**, *23*, 6930.
- (9) Su, Y.; Wang, X.; Li, Y.; Song, Y.; Sui, Y.; Wang, X. *Angew. Chem., Int. Ed.* **2015**, *54*, 1634.
- (10) Figueira-Duarte, T. M.; Müllen, K. *Chem. Rev.* **2011**, *111*, 7260.
- (11) (a) Kitagawa, Y.; Saito, T.; Ito, M.; Shoji, M.; Koizumi, K.; Yamanaka, S.; Kawakami, T.; Okumura, M.; Yamaguchi, K. *Chem. Phys. Lett.* **2007**, *442*, 445. (b) Saito, T.; Nishihara, S.; Kataoka, Y.; Nakanishi, Y.; Matsui, T.; Kitagawa, Y.; Kawakami, T.; Okumura, M.; Yamaguchi, K. *Chem. Phys. Lett.* **2009**, *483*, 168.
- (12) The large singlet–triplet gap of $1^{••2-}$ makes it difficult to be thermally excited to an amount detectable by EPR spectroscopy. However, the presence of a small amount of a thermally excited triplet state makes the diradical NMR silent at room temperature and 213 K.
- (13) Due to the lack of anisotropic splitting observed in the spectra despite several measurements under different conditions, we were not able to determine the zero-field parameters.
- (14) Kostenko, A.; Tumanskii, B.; Karni, M.; Inoue, S.; Ichinohe, M.; Sekiguchi, A.; Apeloig, Y. *Angew. Chem., Int. Ed.* **2015**, *54*, 12144.